Conjecture of a parity law regarding the singlet-triplet gap in graphitic ribbons

Mohamad Al Hajj, Fabien Alet, Sylvain Capponi, Marie-Bernadette Lepetit, Jean-Paul Malrieu

EPJ manuscript No.
(will be inserted by the editor)

Conjecture of a parity law regarding the singlet-triplet gap in graphitic ribbons

Mohamad Al Hajj[(a)], Fabien Alet[(b)], Sylvain Capponi[(b)], Marie Bernadette Lepetit[(c)] and Jean-Paul Malrieu[(a)]

(*a*) laboratoire de Chimie et Physique Quantique, IRSAMC/UMR5626, Université Paul Sabatier, 118 route de Narbonne, F-31062 Toulouse Cedex 4, France
(*b*) laboratoire de Physique Théorique, IRSAMC/UMR5152, Université Paul Sabatier, 118 route de Narbonne, F-31062 Toulouse Cedex 4, France
(*c*) CRISMAT, 6 Bd Maréchal Juin, F-14050 Caen Cedex, France

Abstract. This work explores the possibility to transfer the parity law of the singlet-triplet gap established for square ladders (gapped for even number of legs, gapless for odd number of legs) to fused polyacenic 1-D systems, i.e., graphite ribbons. Qualitative arguments are presented in favor of a gapless character when the number n_ω of legs is odd. A series of numerical calculations (quantitative mapping on spin 1/2 chains, renormalized excitonic treatments and Quantum Monte Carlo) confirm the parity law and the gapless character of the ribbon for even n_ω.

PACS. 71.10.-W Theories and models of many-electron systems 71.15.Nc Total energy and cohesive energy calculations 75.10.-b General theory and models of magnetic ordering

1 Introduction

In the recent past the properties of some quasi 1-D strongly correlated materials, namely cuprate ladders, have attracted much interest from solid state physicists. As a major result they have established that the spin gap (i.e., lowest singlet to triplet excitation energy) of the ladders presents a parity law: the ladders are gapped (have a finite excitation energy) when the number of legs is even, and gapless (degenerate singlet and triplet state) for odd number of legs [1]. This result is not evident, since one may consider the ladders as intermediate between the simple 1-D chain and the square 2-D lattice, which are both gapless. Finite ribbons of fused polyacenes (with CH bonds on the most external doubly-bondel carbons) can be seen as organic analogs of the cuprate ladders. They are quasi 1-D fragments of graphite, which is gapless. The non-dimerized linear polyene is also known to be gapless. Are the fused polybenzenoïd ribbons always gapless ?

Although the π-electrons of the conjugated hydrocarbons are not strongly correlated, it has been shown twenty years ago that they can be treated accurately through Heisenberg Hamiltonians, i.e., as spins interacting through AF couplings [2,3]. This view of π-electron systems offers simple rationalizations of many of their properties. A geometry-dependent Heisenberg Hamiltonian has been extracted from accurate calculations of the singlet and $\pi \rightarrow \pi^*$ triplet states of ethylene and happens to be a quantitative tool for the ground and lowest excited states of conjugated hydrocarbons [2,3]. The MM-VB method widely used by Robb and coworkers [4] for the study of their photochemistry is nothing but a π-electron Heisenberg Hamiltonian plus a σ-bond potential. A few years ago density matrix renormalization group (DMRG) calculations have been reported, concerning the singlet-triplet gap of the simplest polyacenic chain, built of aligned fused benzene rings [5]. The extrapolated calculated gap is finite and close to $0.1J$ where J is the spin coupling between adjacent atoms. Actually the polyacene can be viewed as a two-leg ladder in which one rung over two has vanished (cf. figure 1). One might wonder wether there is a similarity between the three-leg ladder and a fused polyacenic infinite ribbon with two ranks of benzene rings. From qualitative arguments one may conjecture that the singlet-triplet

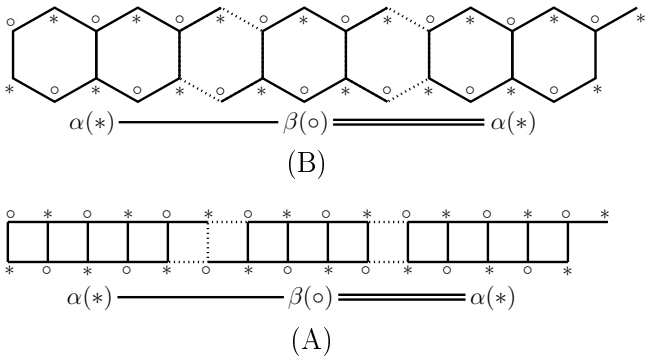

Fig. 1. Two-leg ladder (A) and $n_\omega = 1$ fused polyacene (B), and their mapping into spin 1/2 chains.

excitation in such polyacenic ribbons of graphite is finite when the number of superposed rings in the width of the ribbon, n_ω, is odd and vanishes when n_ω is even. Numerical calculations using the quantitative mapping on known 1-D chains, renormalized excitonic method (REM) [6], density matrix renormalization group [7,8] technique and quantum Monte Carlo calculations (QMC), show that the gap vanishes for even n_ω but is non-zero for odd n_ω ribbons.

2 Qualitative arguments

Qualitative arguments can be used to rationalize the parity law of ladders, which can also be applied to 1-D fused polyacenes. They are based on the real-space renormalization group (RSRG), originally proposed by Wilson [9]. Concerning spin lattices one may consider that they are built from blocks rather than from sites. Of course these blocks interact. If the blocks do not have a singlet ground state, but a doublet, or a triplet, they can be seen as interacting effective spins [10]. A quasi 1-D lattice can then be easily transformed [11] into a simple 1-D spin chain, the properties of which are well known. Considering 2-leg ladders, one may define $(2N_s+1)$ sites blocks, which have a ground state doublet ($S_Z = \pm 1/2$). But these blocks do not have equal interactions with their left and right nearest neighbors (cf. figure 1 (A)). The 2-leg ladder maps into a *dimerized* (i.e., bond-alternated) spin chain, which is known to present a gap. An alternative partition uses blocks with even number of sites (figure 2 (A)). Such a chain of $S = 1$ spins is known to present the so-called Haldane gap [12]. Both partitions predict a gap.

If one applies the same arguments to the $n_\omega = 1$ polyacenic chain one obtains a similar mapping pictured in figure 1 (B). The partition into blocks of $(4N_S + 1)$ sites and $(4N_S + 3)$ sites produces an alternating dimerized spin chain, which is gapped. The partition into $4N_S$ sites blocks with triplet ground states (figure 2) leads to a Haldane gap [12]. Both partitions suggest a finite excitation energy.

The ladder with odd number of legs can be partitioned into blocks with odd number of sites which have equal interactions with the left and right neighbors, and the ladders is mapped into a non-dimerized gapless 1-D chain,

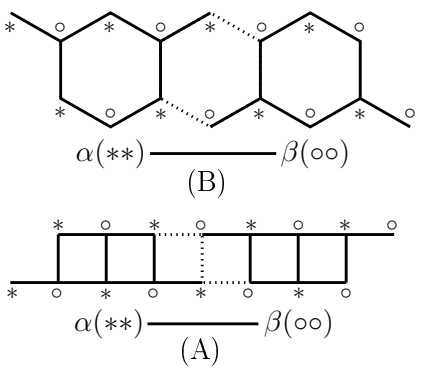

Fig. 2. Mapping of ladder and polyacene into a spin-1 chain.

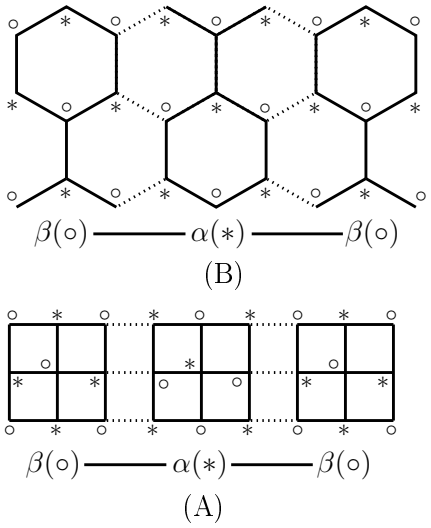

Fig. 3. Three-leg ladder (A) and $n_\omega = 2$ fused polyacene (B), and their mapping into spin 1/2 chains.

(cf. figure 3 (A)). For the $n_\omega = 2$ polybenzenoïd ribbon the simplest partition defines 9-site blocks presenting a $S = 1/2$ ground state and equal anti-ferromagnetic (AF) interactions with left and right nearest neighbors (cf. figure 3 (B)). As an AF non-dimerized chain the $n_\omega = 2$ polyacenic ribbon should not be gapped. It is quite easy to generalize these various mappings to $n_\omega = 3$ or 4 ribbons.

The arguments can easily be generalized to any thickness of the ribbon according to figure 4, which proposes a mapping into a non-dimerized $S = 1/2$ spin chain for odd values of n_ω and into an integer-S non-dimerized spin chain for even n_ω. Of course the $S = 1$ chain may be transformed into a dimerized chain of $S = 1/2$ blocks by shifting one external carbon from one block to its right side neighbor block.

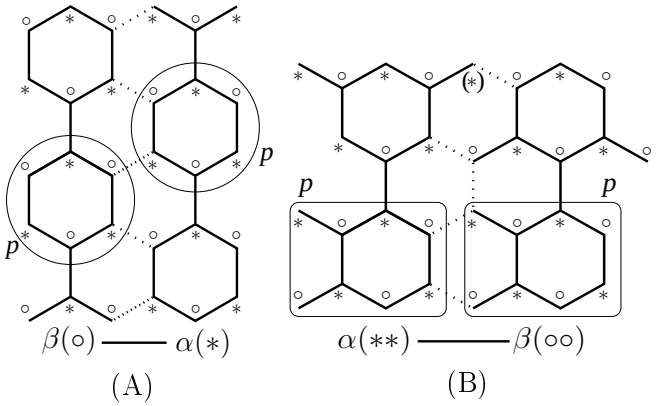

Fig. 4. Generalization of the mappings in non-dimerized AF $S = 1/2$ chains for $n_\omega = 2p + 3$ (A) and $S = 1$ chains for $n_\omega = 2p + 2$ (B). Moving the $(*)$ atom the right-side blocks produces a dimerized $S = 1/2$ AF chains.

3 Numerical studies

Numerical verifications of that conjecture have been tempted for $n_\omega = 1, 2$ and 3. Several techniques have been employed

3.1 Mapping into 1-D chains

For $n_\omega = 1$ the chain may be considered as built from A and B blocks of 7 and 9, 9 and 11 or 11 and 13 sites, according to figure 1 (B). One obtains then a dimerized $S = 1/2$ spin chain with different values J_1, J_2 between the $A-B$ and $B-A$ blocks. A previons study of the dimerized $S = 1/2$ chain has suggested that the gap follows the law

$$\Delta E = (J_1 + J_2)\delta^{0.71} \text{ with } \delta = \frac{(J_1 - J_2)}{(J_1 + J_2)}. \qquad (1)$$

Applying equation 1 one obtains

$$\Delta E = 0.097J \text{ for the (7-9) blocks,}$$
$$\Delta E = 0.116J \text{ for the (9-11) blocks,}$$
$$\Delta E = 0.120J \text{ for the (11-13) blocks,}$$

hence a finite gap.

For $n_\omega = 2$ the simple mapping into a non-dimerized $S = 1/2$ AF spin chain of 9-site blocks (cf. figure 3 (B)) pleads in favor of a non-gapped character, but this hypothesis rests on the neglect of the effective interaction between next-nearest-neighbor blocks. Actually a non-dimerized AF chain becomes gapped when the ratio J'_{NNN}/J_{NN} is larger than 0.22 [13]. We have extracted the effective couplings between 9-site blocks (figure 3 (B)) from the exact spectrum of the trimer of blocks and we found a an AF coupling between NN blocks $J_{NN} = 0.15896$ (in good agrument with the value extracted from the dimer $J_{NN} = 0.16622$) and a surpirsingly large ferromagnetic $J'_{NNN} = -0.1705$ coupling. Since an AF $S = 1/2$ chain with ferromagnetic coupling between NNN sites in not gapped, the n_ω ribbon should be gappless.

For $n_\omega = 3$ one may define a dimerized AF $S = 1/2$ chain of 13 and 11 sites respectively as pictured in figure 5. One obtains two values of the inter block AF coupling ($J_1 = 0.180$, $J_2 = 0.094$). Using equation 1 one obtains $\Delta E(n_\omega) = 0.018J$.

3.2 Renormalized excitonic calculations

The recently proposed renormalized excitonic method [6] is based again on a partition into blocks, but the blocks ABC now have an even number of sites, a singlet ground state ψ^0_A and a triplet lowest excited state ψ^*_A. One defines a model space for the AB dimers, spanned by local singly excited states $\psi^*_A\psi^0_B$ and $\psi^0_A\psi^*_B$. Knowing the spectrum of the AB dimer it is possible to define [14]

- the effective energy of $\psi^*_A\psi^0_B$ and $\psi^0_A\psi^*_B$,
- the effective interaction between them.

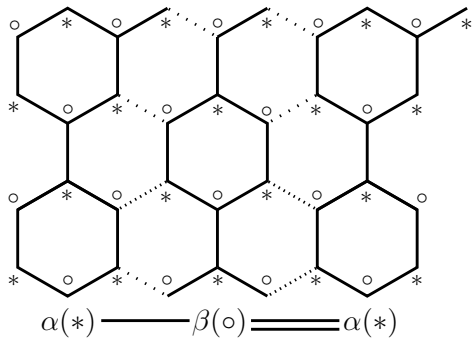

Fig. 5. Definition of the blocks for a mapping into a dimerized $S = 1/2$ chain of $n_\omega = 3$ ribbon.

These informations allow one to apply the excitonic method. For the infinite lattice, this method leads to the following expressions of the excitation energy calculated from N_S sites blocks

$$\Delta E^\infty(N_S) = 2\Delta E(2N_S) - \Delta E(N_S). \qquad (2)$$

The method has been applied elsewhere [11] from 8 sites and 12 sites blocks to 2-leg ladders and the extrapolated gap is $0.47J$, which compares with the best QMC calculation ($0.50J$) [15]. It can be applied to $n_\omega = 1$, $n_\omega = 2$ and $n_\omega = 3$ polybenzenoïd ribbons using the design of the blocks pictured in figure 6.

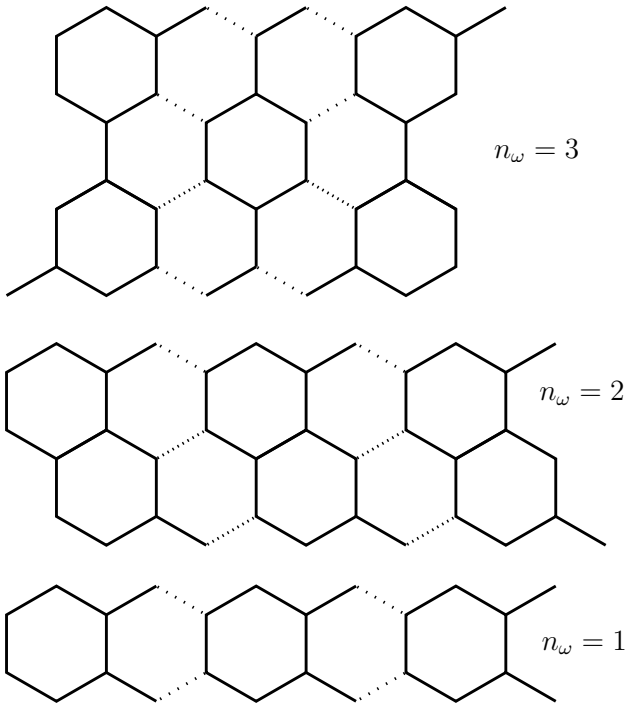

Fig. 6. Definition of blocks for the calculation of the energy gap through the REM.

The calculated gap for $n_\omega = 1$ polyacene is finite. We find

$$\Delta E^\infty(8) = 0.068J \text{ for } N_S = 8 \text{ sites blocks},$$
$$\Delta E^\infty(12) = 0.094J \text{ for } N_S = 12 \text{ sites blocks}.$$

Since the N_S^{-1} composants of the excitation energy disappears in the expression of $\Delta E^\infty(N_S)$, an extrapolation in terms of N_S^{-2} leads to $\Delta E = 0.103J$.

The result of the REM method for the $n_\omega = 2$ lattice from the $N_S = 12$ sites blocks is one order of magnitude smaller, $\Delta E^\infty(12) = 0.013J$. Extrapolation is not possible in this problem, but this result strongly supports our conjecture that this fused polybenzenoïd ribbon is not gapped or presents a very weak gap.

For $n_\omega = 3$ unequal blocks of $N_S = 14$ and $N_S = 10$ sites have been used, according to figure 6. Since the blocks are different it is necessary to generalize the algebra of ref. 6, as performed in the Appendix. The final result is $\Delta E^\infty(14, 10) = 0.0125J$, i.e., close to the previously calculated gap for $n_\omega = 2$. One may say that these calculations at least support the idea of a strong constrast between the odd and even ribbons.

3.3 Density matrix renormalization group

DMRG calculations had been performed [5] for $n_\omega = 1$, giving a gap which ranges between of 0.097 and $0.112J$. The application of this method to thicker ribbons, $n_\omega = 2$ or 3, is rather difficult since the frontier between the left and right blocks involves an increasing number of sites and therefore of states in the frontier domain. The results for $n_\omega = 2$ do not depend signficantly on the number of states kept, but the calculated gaps signficantly differ from those given by other methods.

$$\Delta E = 0.042J \text{ for } n_\omega = 2,$$
$$\Delta E = 0.141J \text{ for } n_\omega = 3,$$

These results confirm a strong alternation but for $n_\omega = 3$ it is one order of magnitude larger than those of REM and QMC. We therefore believe that such thick quasi 1-D systems are hardly tractable by DMRG.

3.4 Quantum Monte Carlo

We now present Quantum Monte Carlo results for the $n_w = 1, 2$ and 3 ribbons. As the spin lattices are not frustrated, efficient QMC algorithms are available which allow to simulate with high-precision large systems, at finite albeit extremely small temperatures. Here we use a multi-cluster continuous time [16] loop algorithm [17] which is free of any systematic errors. We simulate systems of size up to length $L = 800$ (the total number of spins is $N_s = 2(n_\omega + 1)L$) and at inverse temperature up to $\beta.J = J/T = 1000$. To determine the gapfull/gapless nature of the systems, we calculate the correlation length

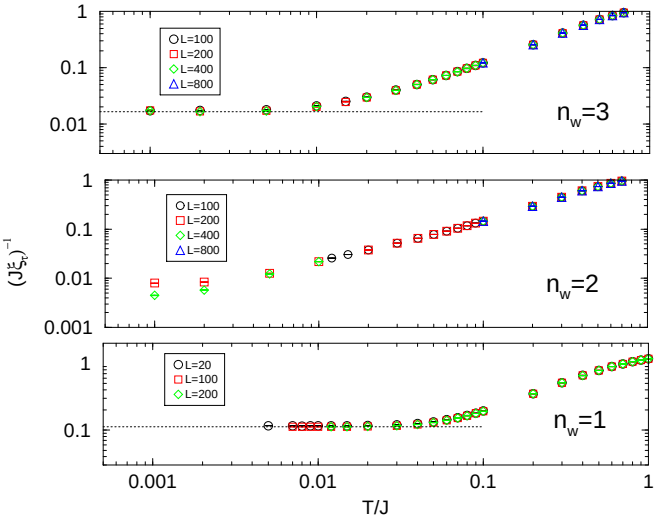

Fig. 7. Quantum Monte Carlo results for the inverse of the imaginary time correlation length as a function of temperature for the $n_\omega = 1$ (bottom pannel), $n_\omega = 2$ (middle pannel) and $n_\omega = 3$ (top pannel), for different system sizes L. Values of the extracted gaps $\Delta(n_\omega = 1) = 0.1122(4)J$ and $\Delta(n_\omega = 3) = 0.0165(5)J$ are represented by dashed-lines for $n_\omega = 1$ and 3.

in imaginary time ξ_τ with the help of a standard second moment estimator [18,19]

$$\xi_\tau = \frac{\beta}{2\pi}\left(\frac{\chi(\omega = 0)}{\chi(\omega = 2\pi/\beta)} - 1\right)^{1/2} \quad (3)$$

where $\chi(\omega) = \int_0^\beta d\tau e^{i\omega\tau}\chi(\tau)$ is the Fourier-transform of the imaginary time dynamical antiferromagnetic structure factor $\chi(\tau) = \frac{1}{\beta N_s^2}\sum_{i,j}(-)^{r_j - r_i}\int_O^\beta dt S_i^z(t)S_j^z(t+\tau)$. $\chi(\omega)$ is measured with an improved estimator [20]. It can be shown that for a gapped system, ξ_τ converges to the inverse spin gap in the thermodynamic limit at zero temperature : $\lim_{L,\beta\to\infty}\xi_\tau(L,\beta) = \Delta^{-1}$. On the other hand, when the system is gapless, ξ_τ^{-1} is an upper bound of the finite-size gap for any finite L and β. In fig. 7, we represent the inverse of the imaginary correlation length $(J\xi_\tau)^{-1}$ as a function of the temperature T/J in log-log scale, for the three types of ribbon $n_\omega = 1, 2$ and 3. This representation is useful to see if the system is gapped as $(J\xi_\tau)^{-1}$ saturates at low temperatures to the gap value Δ/J.

For $n_\omega = 1$, $(J\xi_\tau)^{-1}$ clearly converges at low T to a minimum value identical for system sizes $L = 100$ and $L = 200$, indicating that finite-size effects are absent. From the results for the largest L at the lowest T, we extract the value of the spin gap $\Delta(n_\omega = 1) = 0.1122(4)J$, in perfect agreement with DMRG calculations [5].

We find no saturation of $(J\xi_\tau)^{-1}$ at the lowest temperature for the largest system size $L = 400$ studied for $n_\omega = 2$. Data for smaller systems ($L = 100, 200$) present signs of saturation at low enough T towards values which depend on the system size: this is naturally interpreted as the signature of finite-size gaps. Strictly speaking, the numerical data for the largest L at the lowest $T = 0.001$ can only put an upper bound $\Delta(n_\omega = 2) < 0.0045J$ on

the value of the gap. However, The general form of the T dependence of $(J\xi_\tau)^{-1}$ and the fact that we still have finite-size effects for large systems at low T naturally indicate that the $n_\omega = 2$ system is gapless $\Delta(n_\omega = 2) = 0$.

Finally for $n_\omega = 3$, a convergence of $(J\xi_\tau)^{-1}$ is recovered at low enough T towards a size-independent constant. As for the $n_\omega = 1$ case, this indicates that the system is gapped and we obtain the gap value $\Delta(n_\omega = 3) = 0.0165(5)J$. Please note that we had to resort to large systems at very low temperatures ($L = 800$ and $T = 0.001$) to assert the complete convergence of our data: this is ascribed to the small value of the gap (an order of magnitude lower than for $n_\omega = 1$).

In conclusion, the QMC simulations unambiguously proove the even/odd number of legs effect for the gapfull/gapless nature of 1-D fused polyacenic ribbons. As for spin ladders, we find that the value of the gap decreases with the number of legs for the even legs (odd n_ω) ribbons.

4 Conclusion

The conjecture of the existence of parity law concerning the spin gap in polygbenzenoïd ribbons was based on reasonable qualitative arguments. This conjecture seems to be confirmed by a consistent set of numerical calculations summarized in table 1. The DMRG does not seem reliable for the thick quasi 1-D ribbons. The REM fails to give a zero gap for $n_\omega = 2$ but indicates a contrast between odd and even ribbons. The quantitative mapping and the accurate QMC calculations confirm the gapless character of the $n_\omega = 2$ ribbons and agree on the amplitude of the gap for $n_\omega = 1$ and $n_\omega = 3$. For graphite ribbons, for which $J \sim 2.2$eV at the typical r_{cc} distance (1.395Å), the gaps should be close to 0.23eV for $n_\omega = 1$ and 0.03eV for $n_\omega = 3$.

	Mapping	REM	DMRG	QMC
$n_\omega = 1$	0.120	0.103	0.097-0.112	0.115
$n_\omega = 2$	0	0.013	(0.042)	0
$n_\omega = 3$	0.012	0.012	(0.141)	0.015

Table 1. Calculed gaps (in J units) obtained from different methods

A Renormalized excitonic method for an $(A-B)_n$ chain

One has two types of blocks A and B. The ground and lowest excited eigenfunctions for each block are given by

$$H_A|\psi_A^0\rangle = E_A^0|\psi_A^0\rangle, \quad (4)$$
$$H_A|\psi_A^*\rangle = E_A^*|\psi_A^*\rangle, \quad (5)$$
$$H_B|\psi_B^0\rangle = E_B^0|\psi_B^0\rangle, \quad (6)$$
$$H_B|\psi_B^*\rangle = E_B^*|\psi_B^*\rangle. \quad (7)$$

The ground state of the chain is represented by

$$\Psi^0 = \prod_i \psi_{A_i}^0 \prod_j \psi_{B_j}^0. \quad (8)$$

Its energy will be

$$\langle\Psi^0|H^{eff}|\Psi^0\rangle = n(E_A^0 + E_B^0) + n(v_{AB} + v_{BA}). \quad (9)$$

The interaction energies between two adjacent blocks is given by the knowledge of the exact energies of the AB and BA dimers

$$H_{AB}|\Psi_{AB}^0\rangle = E_{AB}^0|\Psi_{AB}^0\rangle, \; E_{AB}^0 = E_A^0 + E_B^0 + v_{AB}. \quad (10)$$

For the description of excited states one needs to estimate the effective interaction between a local excited state and the neighbor ground states and the integral responsable for the transfer of excitation. These informations are obtained from the excited solutions of the dimers. One shall especially consider the two eigenstates

$$H_{AB}|\Psi_{AB}^*\rangle = E_{AB}^*|\Psi_{AB}^*\rangle, \quad (11)$$
$$H_{AB}|\Psi_{AB}^{*'}\rangle = E_{AB}^{*'}|\Psi_{AB}^{*'}\rangle, \quad (12)$$

having the largest projections $|\tilde{\Psi}_{AB}^*\rangle$ and $|\tilde{\Psi}_{AB}^{*'}\rangle$, on the model space spanned by $\psi_A^*\psi_B^0$ and $\psi_A^0\psi_B^*$, which can be written after orthogonalization as

$$|\tilde{\Psi}_{AB}^*\rangle = \lambda|\psi_A^*\psi_B^0\rangle + \mu|\psi_A^0\psi_B^*\rangle, \quad (13)$$
$$|\tilde{\Psi}_{AB}^{*'}\rangle = -\mu|\psi_A^*\psi_B^0\rangle + \lambda|\psi_A^0\psi_B^*\rangle. \quad (14)$$

It results that

$$\langle\psi_A^*\psi_B^0|H^{eff}|\psi_A^*\psi_B^0\rangle = \lambda^2 E_{AB}^* + \mu^2 E_{AB}^{*'} = E_A^* + E_B^0 + v_{(A^*)B}, \quad (15)$$
$$\langle\psi_A^0\psi_B^*|H^{eff}|\psi_A^0\psi_B^*\rangle = \mu^2 E_{AB}^* + \lambda^2 E_{AB}^{*'} = E_A^0 + E_B^* + v_{A(B^*)}, \quad (16)$$
$$\langle\psi_A^*\psi_B^0|H^{eff}|\psi_A^0\psi_B^*\rangle = (E_{AB}^* - E_{AB}^{*'})\lambda\mu = h_{AB}. \quad (17)$$

For the periodic system the delocalized excited states will be respresented as linear combinations of localy excited states on either A or B blocks

$$\Psi_{A_m}^* = \psi_{A_m}^* \prod_{i\neq m} \psi_{A_i}^0 \prod_j \psi_{B_j}^0, \quad (18)$$
$$\Psi_{B_n}^* = \psi_{B_n}^* \prod_{j\neq n} \psi_{B_j}^0 \prod_i \psi_{A_i}^0, \quad (19)$$

The energies of $\Psi_{A_m}^*$ and $\Psi_{B_n}^*$ are given by

$$\langle\Psi_{A_m}^*|H^{eff}|\Psi_{A_m}^*\rangle - \langle\Psi^0|H^{eff}|\Psi^0\rangle = E_A^* - E_A^0 + v_{(A^*)B} - v_{AB}, \quad (20)$$
$$\langle\Psi_{B_n}^*|H^{eff}|\Psi_{B_n}^*\rangle - \langle\Psi^0|H^{eff}|\Psi^0\rangle = E_B^* - E_B^0 + v_{(B^*)A} - v_{BA}, \quad (21)$$

This locally excited state are coupled with the states locally excited on the adjacent B blocks

$$\langle\Psi_{A_m}^*|H^{eff}|\Psi_{B_m}^*\rangle = h_{AB}. \quad (22)$$

For the lowest state of the lattice, corresponding to $\overrightarrow{k} = 0$, the delocalized excited states can be written as a linear combination of

$$(\Psi_a^*)_{\overrightarrow{k}=0} = \frac{1}{\sqrt{N}} \sum_{A_m} \Psi_{A_m}^*, \tag{23}$$

and

$$(\Psi_b^*)_{\overrightarrow{k}=0} = \frac{1}{\sqrt{N}} \sum_{B_n} \Psi_{B_n}^*, \tag{24}$$

solution of a 2×2 matrix whose elements are

$$\left\langle (\Psi_a^*)_{\overrightarrow{k}=0} \middle| H^{eff} \middle| (\Psi_a^*)_{\overrightarrow{k}=0} \right\rangle - \left\langle \Psi^0 \middle| H^{eff} \middle| \Psi^0 \right\rangle = E_A^* - E_A^0 + 2\Big(V_{(A^*)B} - V_{AB}\Big), \tag{25}$$

$$\left\langle (\Psi_b^*)_{\overrightarrow{k}=0} \middle| H^{eff} \middle| (\Psi_b^*)_{\overrightarrow{k}=0} \right\rangle - \left\langle \Psi^0 \middle| H^{eff} \middle| \Psi^0 \right\rangle = E_B^* - E_B^0 + 2\Big(V_{(B^*)A} - V_{BA}\Big), \tag{26}$$

$$\left\langle (\Psi_a^*)_{\overrightarrow{k}=0} \middle| H^{eff} \middle| (\Psi_b^*)_{\overrightarrow{k}=0} \right\rangle = 2h_{AB}. \tag{27}$$

References

1. S. R. White, R.M. Noack, and D. J. Scalapino, Phys. Rev. Lett. **73**, 886 (1994).
2. M. Said, D. Maynau, J.-P. Malrieu, and M. A. G. Bach, J. Am. Chem. Soc. **106**, 571 (1984).
3. M. Said, D. Maynau, and J.-P. Malrieu, J. Am. Chem. Soc. **106**, 580 (1984).
4. F. Jolibois, M. J. Bearpark, S. Klein, M. Olivucci, and M. A. Robb, J. Am. Chem. Soc. **122**, 5801 (2000).
5. Y. Gao, C.-G. Liu, and Y.-S. Jiang, J. Phys. Chem. A **106**, 2592 (2002).
6. M. Al Hajj, J.-P. Malrieu, and N. Guihéry, Phys. Rev. B **72**, 224412 (2005).
7. S. R. White, Phys. Rev. Lett. **69**, 2863 (1992).
8. S. R. White, Phys. Rev. B **48**, 10345 (1993).
9. K.G Wilson, Rev. Mod. Phys. **47**, 773 (1975).
10. J.-P. Malrieu and N. Guihéry, Phys. Rev. B **63**, 085110 (2001).
11. M. Al Hajj, N. Guihéry, J.-P. Malrieu, and B. Bocquillon, Eur. Phys. J. B **41**, 11 (2004).
12. F. D. M. Haldane, Phys. Lett. A **93**, 464 (1983).
13. S. Eggert, Phys. Rev. B **54**, 9612 (1996).
14. C. Bloch, Nucl. Phys. **6**, 329 (1958).
15. M. Greven, R. J. Birgeneau, and U.-J. Wiese, Phys. Rev. Lett. **77**, 1868 (1996).
16. B.B. Beard and U.-J. Wiese, Phys. Rev. Lett. **77**, 5130 (1996).
17. H.G. Evertz, G. Lana and M. Marcu, Phys. Rev. Lett. **70**, 875 (1993).
18. F. Cooper, B. Freedman and D. Preston, Nucl. Phys. B **210**, 210 (1982).
19. S. Todo and K. Kato, Phys. Rev. Lett. **87**, 047203 (2001).
20. G.A. Baker, Jr. and N. Kawashima, Phys. Rev. Lett. **75**, 994 (1995).
21. F. Alet *et al.*, J. Phys. Soc. Jap. Suppl. **74**, 30 (2005); M. Troyer, B. Ammon and E. Heeb, Lect. Notes Comput. Sci., **1505**, 191 (1998). See also `http://alps.comp-phys.org`.